SRNL-STI-2009-00763
Rev. 0

DESTRUCTIVE EXAMINATION OF SHIPPING PACKAGE 9975-02028

W. L. Daugherty
T.M. Stefek

Savannah River National Laboratory
Materials Science & Technology

Publication Date: December 2009

Savannah River Nuclear Solutions
Savannah River Site
Aiken, SC 29808

This document was prepared in conjunction with work accomplished under Contract No. DE-AC09-08SR22470 with the U.S. Department of Energy.

DISCLAIMER

DESTRUCTIVE EXAMINATION OF SHIPPING PACKAGE 9975-02028

APPROVALS:

W. L. Daugherty _____ Date _____
Author, Materials Science and Technology

T. M. Stefek _____ Date _____
Author, Materials Science and Technology

T. E. Skidmore _____ Date _____
Technical Review, Materials Science and Technology

K. A. Dunn _____ Date _____
Pu Surveillance Program Lead, Materials Science and Technology

G. T. Chandler _____ Date _____
Manager, Materials App & Process Tech

E. R. Hackney _____ Date _____
NMM Engineering

REVIEWS:

J. L. Murphy _____ Date _____
Savannah River Packaging Technology

J. W. McEvoy _____ Date _____
9975 Shipping Package Design Authority

Revision Log

Document No. SRNL-STI-2009-00763 **Rev. No.** 0

Document Title Destructive Examination of Shipping Package 9975-02028

Rev. #	Page #	Description of Revision	Date
0	all	Original document	11/ /2009

Nomenclature

ASTM – American Society for Testing and Materials

DSA – Documented Safety Analysis

FT-IR – Fourier Transform Infrared Spectroscopy

ID – Inside Diameter

KAC – K-Area Complex

OD – Outside Diameter

PCV - Primary Containment Vessel

RH – Relative Humidity

SAT – Satisfactory

SCV – Secondary Containment Vessel

SEM – Scanning Electron Microscope

SPA – Surveillance Program Authority

SRNL – Savannah River National Laboratory

SRS – Savannah River Site

UNSAT – Unsatisfactory

WME – Wood Moisture Equivalent

Destructive Examination of Shipping Package 9975-02028

Summary

Destructive and non-destructive examinations have been performed on specified components of shipping package 9975-02028. For those attributes that were also measured during the field surveillance, no significant changes were observed. Four conditions were identified that do not meet inspection criteria. These conditions are subject to additional investigation and disposition by the Surveillance Program Authority. The conditions include:

- The lead shield was covered with a white corrosion layer.
- The lead shield height exceeds drawing requirements.
- Mold was observed on the lower fiberboard subassembly.
- Fiberboard thermal conductivity in the axial direction exceeded the specified range.

The Surveillance Program Authority was notified of these conditions and will document the disposition by surveillance report. All other observations and test results met identified criteria, or were collected for information and trending purposes.

Introduction

The Savannah River Site (SRS) stores packages containing plutonium (Pu) materials in the K-Area Complex (KAC). The Pu materials are packaged per the DOE 3013 Standard and stored within Model 9975 shipping packages in KAC.

The KAC facility DSA (Document Safety Analysis) [1] credits the Model 9975 package to perform several safety functions, including criticality prevention, impact resistance, containment, and fire resistance to ensure the plutonium materials remain in a safe configuration during normal and accident conditions. The Model 9975 package is expected to perform its safety function for at least 12 years from initial packaging. The DSA recognizes the degradation potential for the materials of package construction over time in the KAC storage environment and requires an assessment of materials performance to validate the assumptions of the analysis and ultimately predict service life.

As part of the comprehensive Model 9975 package surveillance program [2-3], destructive examination of package 9975-02028 was performed following field surveillance in accordance with Reference [4]. Field surveillance of the Model 9975 package in KAC included nondestructive examination of the drum, fiberboard, lead shield and containment vessels [5]. Results of the field surveillance are provided in Attachment 1.

Package History

Fabrication of package 9975-02028 was completed by Accurate Machine Products Corporation on March 27, 2003. The package contained plutonium oxide material from Rocky Flats packaged in accordance with DOE-STD-3013. RFETS loaded and shipped this package on May 22, 2003. It was received at KAC on August 15, 2004. Routine field surveillance was performed on July 6, 2009. SRNL received the package on July 9, 2009 and performed destructive examination activities between August 19 and October 13, 2009.

Discussion

The results of the field surveillance [6] were reviewed. No unsatisfactory conditions were noted. As the package was opened, and components removed, each component was marked to identify its orientation within the package. For components that were removed during the field surveillance, their orientation at the time of this examination probably bears no relation to their orientation while stored in KAC. However, the bottom fiberboard subassembly and lead shield would likely have remained in the same orientation they occupied in KAC.

Examination activities are documented through photographs, data sheets, and other documents. This documentation is maintained in a laboratory notebook [7]. The following examination activities were performed:

Fiberboard physical properties:

The weight and dimensions of the top and bottom fiberboard subassemblies were measured. The weight of the top subassembly was 12.186 kg (26.87 lb). During the field surveillance, the measured weight of the top subassembly was 26.6 lb. These two values suggest a modest increase in weight of the upper subassembly between the two measurements. This might reflect a re-distribution of moisture from the lower subassembly to the upper subassembly following removal of the 3013 container and its associated heat load. Weight and dimension data are recorded in Table 1.

The air shield was cut and peeled back at four locations to permit accurate measurement of the top fiberboard subassembly dimensions. In order to calculate the density of each subassembly, nominal dimensions were assumed for the aluminum bearing plate and air shield. The calculated densities (0.27 g/cc top subassembly, 0.29 g/cc bottom subassembly) meet the limit for the criticality control function, 0.21 g/cc minimum [4]. The volume and density were calculated using the following equations (refer to the Table 1 sketch for dimension nomenclature).

Top subassembly fiberboard volume,

$$V_U = (UD1)^2\,(UH1)\,(\pi/4) + [(UD1) - 2\,(UR2)]^2\,(UH2)\,(\pi/4) - (UD2)^2\,(UH3)\,(\pi/4) - 59.96\ \text{inch}^3$$

Top subassembly fiberboard weight, W_U = upper subassembly weight – 9.773 lb

Top subassembly fiberboard density, $\rho_U = W_U / V_U$

Bottom subassembly fiberboard volume,

$$V_L = (LD1)^2\,(LH1)\,(\pi/4) - [(LD2) + 2\,(LR1)]^2\,(LH3)\,(\pi/4) - (LD2)^2\,(LH2)\,(\pi/4) - 59.96\ \text{inch}^3$$

Bottom subassembly fiberboard weight, W_L = bottom subassembly weight – 4.827 lb
Bottom subassembly fiberboard density, $\rho_L = W_L / V_L$

Fiberboard dimensions measured during field surveillance are summarized in Attachment 1, and are consistent with drawing requirements and destructive examination measurements. For each of the five dimensions measured in both the field surveillance and destructive examination, the measured values are similar, but tend to be larger in the destructive examination. This direction of change is consistent with the increased weight and possible increase in moisture content of the upper fiberboard subassembly. No significant observations were found with the fiberboard physical measurements.

Fiberboard visual appearance:

No significant material or physical damage was observed, and layers were well bonded. The lower subassembly came out smoothly without interference, and gaps exist against the drum.

Following removal of both the top and bottom fiberboard subassemblies from the outer drum, both were inspected visually. Although no obvious odor of mold or mildew was noted when opening the package, mold was observed on the lower fiberboard subassembly (Figure 1). Patches of mold were observed across the lower subassembly bottom and in a local region of the lower subassembly OD. Some patches of mold from the bottom of the lower subassembly and fiberboard residue remained adhered to the bottom of the drum (Figure 2). Mold was also initially reported on the upper subassembly, but it was difficult to distinguish from the fiberboard structure. This mold was not apparent in subsequent examination of the upper subassembly, but a slight musty odor was present at that time. The lower fiberboard subassembly contained two local dents that were approximately 0.2 inches deep, and two longer scrape marks on the OD surface. The indentations were located at 280^o and approximately 15 inches from the bottom (Figure 3).

Fiberboard moisture content:

The moisture content of the fiberboard will affect its properties, including density, mechanical strength and thermal properties. Measuring the relative moisture content of the top and bottom subassemblies, and the relative humidity inside the package, provides reference data to potentially correlate laboratory test results with behavior in KAC. In addition to measuring the fiberboard moisture content during destructive examination, measurements were also taken during field surveillance to the extent the fiberboard was accessible.

A GE Protimeter Surveymaster moisture probe was used to measure the relative moisture content of the top and bottom fiberboard subassemblies. This probe identifies the wood moisture equivalent (WME), or the weight % of moisture that would produce the same electrical conductivity in wood. Moisture measurements of both the upper and lower subassemblies were made soon after opening the drum. Moisture content data are presented in Figure 4.

Moisture measurements were compared to those taken during previous destructive examinations [8 - 11]. The readings on 9975-02028 generally fall within the range of reading on previous packages, but the distribution is somewhat different. For the current package lower subassembly values range from 10.5 to 18.7 %WME, with the higher values around the bottom OD. The highest of these values is

greater than observed on previous DE packages. Upper subassembly moisture readings range from 11.1 to 19.0 %WME, with the higher values at the top under the air shield. The higher of these values are also greater than observed on previous DE packages. Another difference from previous DE packages is that the moisture gradient from the ID to OD is ~4-6 %WME, in contrast to the 2 – 4 %WME range typically seen before.

The fiberboard moisture measurements made during field surveillance show agreement on average with the subsequent data. However, they also show a higher moisture gradient across the fiberboard sidewall (Figure 4). The moisture gradient that developed as a result of the internal heat source had decreased slightly during the ~6 weeks between unloading and destructive examination.

Consistent with recent efforts to correlate moisture content of fiberboard with humidity in the surrounding air, several sets of data were taken to correlate these two parameters. The fiberboard was placed back in the drum with a narrow channel cut down the side. A humidity probe was placed in this channel such that it could be raised and lowered with the drum closed. The edge of the drum lid was taped to seal around the gap created by the humidity probe cable. After the humidity came to equilibrium, humidity readings were taken at several elevations along the fiberboard, and the fiberboard was then removed to measure the moisture content at those same locations. This process was repeated several times to show the consistency in the results. These data is summarized in Figure 5. The trendline in this figure highlights the expected relationship of humidity increasing with the moisture content. However, the range of data is too narrow to place much confidence in the magnitude of the trendline slope.

Fiberboard thermal and mechanical properties:

Samples of fiberboard were removed from the bottom fiberboard subassembly to measure compressive strength, specific heat capacity and thermal conductivity. The source location(s) of these samples is illustrated in Figure 6. The thermal conductivity sample from the bottom center of the subassembly is oriented for heat flow in the axial direction (perpendicular to the glue joints). The thermal conductivity sample from the side is oriented for heat flow in the radial direction (parallel to the glue joints). Testing on each sample was performed at a nominal (mean) temperature of approximately 25ºC (77ºF), with no environmental conditioning. Physical data on the fiberboard samples are recorded in Table 2.

The compression test data are shown in Figures 7 and 8, along with select baseline data. For both the perpendicular and parallel orientations, the compression strength of the 9975-02028 samples is similar to the baseline samples conditioned at 77ºF and 70% RH. A series of photographs showing typical compression behavior under parallel loading is shown in Figure 9.

A total of four samples were prepared from the side and base of the lower subassembly for measuring the specific heat capacity of the fiberboard. The specific heat capacity was calculated in accordance with ASTM C351 at a mean temperature of ~25ºC (77ºF). This ASTM Standard specifies test temperatures that would produce a mean test temperature of 60ºC, but allows alternate test temperatures to be substituted as needed. Data were collected for a sample target temperature of 45ºC, and a water temperature of ~5ºC. The sample moisture content was 11.3 – 12.9 % WME (wood moisture equivalent). Each sample was tested three times, and all results were averaged. The average value was 1300 J/kg-K. Multiplying this value by the density of the lower subassembly (286 kg/m^3) gives a heat

capacity of 372,000 J/m^3-K (5.54 Btu/ft^3-F). This meets the required minimum value of 3 Btu/ft^3-F. The specific heat capacity value is consistent with typical baseline laboratory data.

The thermal conductivity of the fiberboard was measured with a Lasercomp Inc. Fox 300 thermal conductivity instrument at a mean temperature of 25ºC (77ºF). For the sample with axial heat flow (perpendicular to the fiberboard layers), the measured thermal conductivity is 0.0626 W/m-K (0.0362 Btu/hr-ft-ºF). This value falls outside the acceptance range identified for destructive examinations (0.025 – 0.035 Btu/hr-ft-ºF [4]). For the sample with radial heat flow (parallel to the fiberboard layers), the measured thermal conductivity is 0.0979 W/m-K (0.0566 Btu/hr-ft-ºF). This value falls within the identified range of 0.053 – 0.067 Btu/hr-ft-ºF [4]. The thermal conductivity values are consistent with typical baseline laboratory data.

Lead shield visual examination:

The entire surface of the lead shield was visually examined. It was found to be free from significant deformation and physical damage, but the outside surface (in contact with the fiberboard) was covered with a white corrosion product (Figure 10). From prior examination of the shield from package 9975-02234, the corrosion product was identified as basic lead carbonate (hydrocerrusite), $Pb_3(CO_3)_2(OH)_2$. No further characterizations of the corrosion product were performed.

Lead Shield Dimensions:

Several lead shield dimensions were measured (Table 3) and all but one are consistent with drawing requirements. The height of the shield (average of 4 measurements) was 24.706 inches, while the drawing specifies a maximum height of 24.7 inches.

The radial thickness was measured near the top of the shield, and was calculated from diametral data taken near the bottom of the shield. The calculated thickness from near the bottom (0.546 inch) is smaller than the measured thickness near the top (0.585 inch). While lead is known to creep at ambient temperatures, these data suggest that no significant creep deformation has occurred thus far, since creep would tend to reduce the thickness near the top relative to the bottom.

O-ring examination and testing:

Prior surveillance testing of the four O-rings from this package included visual examination, dimensional and hardness measurements. Three of these O-rings (SCV outer, PCV outer and PCV inner) received additional testing. All three were submitted for FT-IR spectroscopy to confirm material composition, and the two outer O-rings received optical and SEM microscopic examination of the cross section. The dimensions and weight of the SCV outer and PCV outer O-rings were recorded to calculate their density. The PCV inner O-ring was tensile tested, including a hold point at 50% strain to visually examine the O-ring.

FT-IR spectroscopy generically identified the composition of each O-ring as consistent with a Viton® type fluoroelastomer (Figure 11). Viton® A produces a spectrum nearly identical to Viton® GLT, the base polymer for the specified O-ring compound (Parker Seals V0835-75) and the two are difficult to distinguish by FT-IR analysis alone. Additional test techniques (e.g. dynamic mechanical analysis,

DMA) would be required to uniquely verify the GLT composition. These results are similar to those from previous destructive examination packages [8 - 11] and are consistent with baseline data [12].

As with previous destructive examinations, visual (Figure 12) and SEM (Figure 13) examination of the cross sections identified a distribution of very small particles throughout each O-ring. Each O-ring also had a transition between the inner and outer regions of the cross section, with the center region being slightly coarser in appearance. X-ray analysis on the SEM identified no significant variation in element distribution across this transition. Aside from carbon and fluorine (which are the primary constituents of Viton®) the SEM identified aluminum, silicon, oxygen, zinc, sulfur and calcium. These elements are present in small amounts, and are generally associated with the particles. Though the actual compound is proprietary, zinc, calcium and oxygen are consistent with Viton®-type fluoroelastomer compounds, which typically contain MgO, CaO, $Ca(OH)_2$, ZnO or lead compounds as acid acceptors and heat stabilizers [13]. Aluminum, silicon and sulfur are generally not added to peroxide-cured fluoroelastomer recipes (although there are other sulfur-cured varieties), but may be present as a trace contaminant.

Weight and dimension data for the two outer O-rings are presented in Table 4. The average minor diameter for each O-ring is within the specified tolerances for new O-rings, but the major inside diameter for each O-ring (calculated from the length measured after the O-ring was cut) is greater than specified for new O-rings. This is consistent with a permanent stretch due to the lid diameter. Leak testing during the field surveillance was successful.

The PCV inner O-ring was tensile tested in accordance with ASTM D1414, using a cut (single strand) sample. The test was interrupted at 50% strain to visually examine the O-ring for signs of cracking or other degradation. None were observed. The stress-strain curve for the PCV inner O-ring is shown in Figure 14 along with curves from a new O-ring and from previous destructive examinations. The O-ring from package 9975-02028 displayed tensile properties (strength and elongation) consistent with that observed in previous examinations. The elongation (271%) of this O-ring exceeds the minimum value specified in AMS-R-83485 for new O-rings (120%), while the tensile strength (1.4 ksi) is slightly less than the value specified (1.6 ksi) [12]. While Parker Seals does not change the formulation of these O-rings, there are batch variations.

General:

A general visual examination was performed on all metallic components. Aside from the corrosion of the lead shield (discussed above) no significant damage or degradation was observed, although a small spot (~1/8 inch diameter) on the PCV exterior surface had the appearance of a stain or superficial rust (Figure 15). Several components were observed to have fabrication markings. Various markings were stamped or engraved on the containment vessels and lids (Figure 16). These markings appear to be identification numbers used during manufacture, prior to association of the parts with a final package number.

The distance from the drum flange to the top of the air shield was measured, and ranged from 1.000 to 1.049 inch. The average value was 1.030 inch. The drum drawing [14] identifies a reference value for this dimension as 0.8 inch, and notes that it may vary over time due to variations in fiberboard properties. Pre-operational verification requirements, consistent with fire and drop test qualifications

for the 9975 package, specify this dimension be no greater than 1 inch. During field surveillance, the average value of this dimension (0.982 inch) met this requirement. The increase in this dimension likely resulted during transport of the package to SRNL. The elevated moisture content around the bottom of the lower fiberboard subassembly may have slightly reduced its strength (allowing some initial compaction), and the dynamic conditions of transporting the package to SRNL may have caused additional compaction.

The data from the examination activities described above are compared with field surveillance data in Attachment 1. Several conditions were observed that do not meet specified criteria. The Surveillance Program Authority (SPA) was notified of these conditions, and will direct further investigation and analysis as appropriate. They are summarized as follows:

- The lead shield was covered with a white corrosion layer.
- The lead shield height exceeded drawing requirements.
- Mold was observed on the lower fiberboard subassembly.
- Fiberboard thermal conductivity in the axial direction exceeded the specified range.

Two additional conditions were noted, although they did not violate destructive examination criteria. These are the dimension from the drum flange to the air shield, and the small stain on the PCV. All other observations and examination results are consistent with expectations. All findings will be reviewed by NMM for potential impact on the continued storage of other packages in KAC.

Measurement Uncertainties:

Numerous measurements were made with a variety of instruments during the destructive examination of package 9975-02028. Some of the measurements were specifically compared to inspection criteria, while others were taken for information / trending purposes. All measurements which are compared to inspection criteria were made with calibrated instruments, or were verified against calibrated instruments. The uncertainties associated with measurements and calculated results required to meet inspection criteria are discussed below.

Weight – The weight of each fiberboard subassembly was measured to the nearest 2 grams. The balance used was M&TE, and the calibration data shows an accuracy within 4 grams over the range of interest. A conservative net uncertainty of 6 grams will be used.

Calipers – Three different calipers were used to measure component dimensions. All three calipers are M&TE, and calibration data shows an accuracy within 0.001 inch. In addition, operator bias can affect measurement accuracy through the contact load applied when making a measurement. A degree of give exhibited by the fiberboard will lead to different results as the contact load changes. The larger calipers are judged to be more susceptible to this bias. Metallic components are significantly more rigid than the fiberboard, but operator bias may also exist for those components. While not characterized explicitly, it is judged that the total uncertainty (instrument uncertainty plus operator bias) for fiberboard measurements is no greater than +/- 0.003 inch for the 6 inch calipers, +/- 0.005 inch for the 24 inch calipers, and +/- 0.007 inch for the 40 inch calipers. It is further judged that total uncertainty when measuring metallic components is no greater than +/- 0.003 inch for 6 and 24 inch calipers, and +/- 0.005 inch for the 40 inch calipers.

Manual calipers – Dimension ID2 on the lead shield was captured with manual swing calipers, which was then locked in that position and measured with 24-inch calipers. It is judged that the accuracy of capturing this dimension with the manual calipers is within +/- 0.002 inch, and the measurement of that dimension is then within +/- 0.002 inch, for a (conservatively) combined accuracy of +/- 0.004 inch.

Thermal conductivity instrument – The specifications for the Fox300 thermal conductivity instrument include a stated accuracy of ~1%. Measurement of the thermal conductivity of a calibration standard was accurate to within 1.1%. Prior test reports of fiberboard samples from an independent laboratory, using the same model instrument, identified an overall 3% uncertainty. An uncertainty of 3% will be conservatively assumed for the current measurements.

Heat capacity – The specific heat capacity is derived from temperature and weight measurements, using calibrated instruments. The thermocouple and balance precisions are high. The greatest contribution to error in the specific heat capacity is considered to be consistency of operator technique. The total uncertainty is reflected in the range of results for multiple trials. The heat capacity was measured three times on each of four samples. The variation for each sample ranged from 5 to 28%. The combined uncertainty on the average of 4 samples is 8%.

Where measurement results are used in subsequent calculations, the uncertainty values identified above are assumed to be random. A standard error propagation formula for random errors is used to calculate the final result uncertainty. In some cases, the calculated uncertainty may be less than the potential error from rounding off the result, and the higher variation associated with round-off is reported as the uncertainty. These calculations are documented in the Laboratory Notebook [7]. Calculation results and their uncertainties are summarized as follows:

- Top fiberboard subassembly volume = 28519 +/- 23 cm^3
- Top fiberboard subassembly density = 0.272 +/- 0.001 g/ cm^3
- Bottom fiberboard subassembly volume = 85819 +/- 72 cm^3
- Bottom fiberboard subassembly density = 0.286 +/- 0.001 g/ cm^3
- Shield radial thickness at bottom = 0.546 +/- 0.003 inch
- Thermal conductivity (radial) = 0.0566 +/- 0.002 Btu/hr-ft-ºF
- Thermal conductivity (axial) = 0.0362 +/- 0.001 Btu/hr-ft-ºF
- Heat capacity = 5.5 +/- 0.4 Btu/ft^3-ºF

References

[1] WSRC-SA-2002-00005, Rev. 1CN-7, “K-Area Material Storage Facility Documented Safety Analysis”, June 2008.

[2] SFS-ENG-99-0085, “Summary and Guide to 9975 Container Qualification Program”

[3] WSRC-TR-2001-0286, Rev. 4, “The Savannah River Site Surveillance Program for the Storage of 9975/3013 Plutonium Packages in KAC”, July 2008

[4] WSRC-TR-2005-00135, "Task Technical and Quality Assurance Plan for Destructive Examination of a 9975 Package from Field Surveillance Activities", W. L. Daugherty, April 2005

[5] WSRC-TR-2004-00197, "Inspection Activities and Acceptance Criteria for Field Surveillance of Model 9975 Package O-Rings and Celotex® Materials", W. L. Daugherty, April 2004

[6] SOP-CSS-207-K, Attachment 2 "9975 Surveillance Data Sheet" for surveillance WSRC-SRV-2008-007

[7] WSRC-NB-2008-00002, Laboratory Notebook "9975 Shipping Package Celotex Testing Book III"

[8] WSRC-TR-2005-00273, Rev. 1, "Destructive Examination of Shipping Package 9975-02234", W. L. Daugherty, September 2005.

[9] WSRC-TR-2006-00162, "Destructive Examination of Shipping Package 9975-00826", W. L. Daugherty, May 2006.

[10] WSRC-STI-2007-00558, "Destructive Examination of Shipping Package 9975-00600", W. L. Daugherty, October 2007.

[11] SRNS-STI-2008-00019, "Destructive Examination of Shipping Package 9975-05128", W. L. Daugherty, August 2008.

[12] WSRC-TR-2004-00162, "Baseline Characterization of Model 9975 Shipping Package O-Rings", T. E. Skidmore, March 2004

[13] Rubber Technology Handbook, W. Hofmann, Hanser Publishers, New York, 1989, page 122

[14] Drawing R-R2-F-0025, Rev. 5, "9975 Drum with Flange Closure Subassembly & Details"

Table 1. Fiberboard physical measurements and calculated density

Top Subassembly						
Weight	12.186 kg					R-R2-F-0019 Rev 5
	0/180 deg.		90/270 deg.		Avg.	Nominal value (inch)
UD1 (in)	17.635		17.640		17.638	17.7
UD2 (in)	8.539		8.538		8.538	8.55
	0 deg.	90 deg.	180 deg.	270 deg.	Avg.	
UR1 (in)	3.052	3.057	3.055	3.048	3.053	3.075
UR2 (in)	1.484	1.444	1.445	1.505	1.470	1.5
UH1 (in)	7.074	7.098	7.100	7.080	7.088	7.1
UH2 (in)	2.066	2.074	2.082	2.086	2.077	2.1
UH3 (in)	4.960	4.962	4.969	4.948	4.960	5.0

Top subassembly calculated density = 0.272 g/cc

Bottom Subassembly						
Weight	26.730 kg					R-R2-F-0019 Rev 5
	0/180 deg.		90/270 deg.		Avg.	Nominal value (inch)
LD1 (in)	18.036		18.054		18.045	18.1
LD2 (in)	8.456		8.467		8.462	8.45
	0 deg.	90 deg.	180 deg.	270 deg.	Avg.	
LR1 (in)	3.256	3.258	3.282	3.252	3.262	3.275
LR2 (in)	1.513	1.519	1.515	1.521	1.517	1.55
LH1 (in)	26.630	26.576	26.596	26.632	26.608	26.7
LH2 (in)	20.449	20.441	20.429	20.410	20.432	20.4
LH3 (in)	2.021	2.048	2.032	2.035	2.034	2.0

Bottom subassembly calculated density = 0.286 g/cc

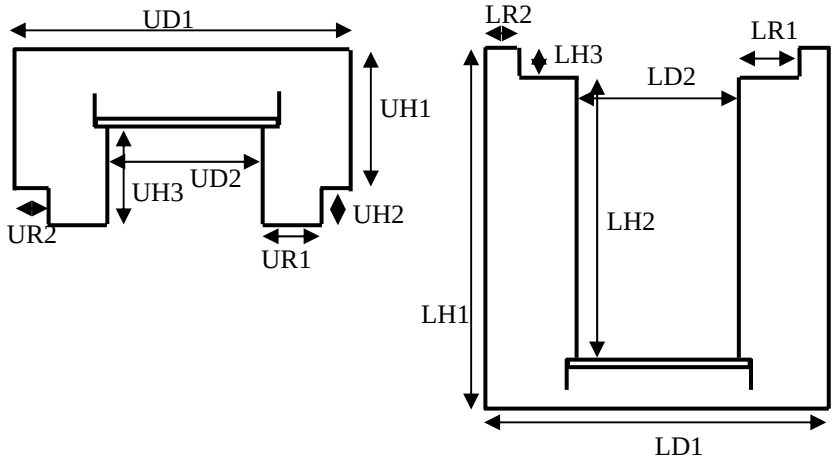

Table 2. Physical data for fiberboard test specimens

Compression Test Sample	Moisture Content (%WME)	Weight (g)	Length (inch)	Width (inch)	Height (inch)	Density (g/cc)
Compression Test Samples						
Side 1 (parallel)	10.9	39.188	2.043	2.042	2.050	0.280
Side 2 (parallel)	10.1	39.365	2.042	2.043	2.047	0.281
Side 3 (perpendicular)	10.9	38.559	2.042	2.050	2.057	0.273
Side 4 (perpendicular)	11.6	38.131	2.042	2.052	2.054	0.270
Base 1 (parallel)	13.0	39.771	2.090	2.064	2.104	0.267
Base 2 (parallel)	12.9	40.358	2.060	2.105	2.108	0.269
Base 3 (perpendicular)	13.1	39.739	2.103	2.031	2.100	0.270
Base 4 (perpendicular)	12.7	39.860	2.102	2.048	2.111	0.268
Thermal Conductivity Samples						
Side (radial)	9.80	428	9.436	6.956	1.493	0.267
Base (axial)	15.1	457	9.516	7.050	1.489	0.279

Table 3. Lead shield dimensions

Dimension	0/180 deg. (inch)		90/270 deg. (inch)		Avg. (inch)	Requirement (inch)
OD (in)	8.340		8.345		8.342	8.252 – 8.35
ID1 (in)	7.251		7.256		7.254	7.25 – 7.26
ID2 (in)	7.252		7.246		7.249	7.24 – 7.26
	0 deg.	90 deg.	180 deg.	270 deg.		
R (in)	0.591	0.566	0.594	0.589	0.585	0.506 min
H (in)	24.709	24.699	24.699	24.717	24.706	24.556 – 24.7

(OD – ID2) / 2 = 0.546 inch

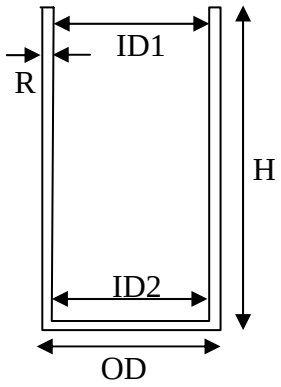

Table 4. O-ring physical data

	PCV Outer O-Ring		SCV Outer O-Ring	
	Radial	Axial	Radial	Axial
Minor Dia. 0 deg	0.1380 inch	0.1350 inch	0.1345 inch	0.1355 inch
Minor Dia. 45 deg	0.1365 inch	0.1350 inch	0.1395 inch	0.1320 inch
Minor Dia. 90 deg	0.1360 inch	0.1350 inch	0.1405 inch	0.1325 inch
Minor Dia. 135 deg	0.1390 inch	0.1340 inch	0.1390 inch	0.1330 inch
Minor Dia. 180 deg	0.1385 inch	0.1350 inch	0.1380 inch	0.1325 inch
Minor Dia. 225 deg	0.1360 inch	0.1345 inch	0.1360 inch	0.1350 inch
Minor Dia. 270 deg	0.1345 inch	0.1350 inch	0.1355 inch	0.1350 inch
Minor Dia. 315 deg	0.1370 inch	0.1350 inch	0.1370 inch	0.1325 inch
Avg. Minor Dia.	**0.1359 inch**		**0.1355 inch**	
Minor Dia. (new)	0.138 +/- 0.006 inch		0.138 +/- 0.006 inch	
Length (after cut)	14 3/64 inch		17 17/64 inch	
Calculated Major Dia.	4.471 inch avg		5.496 inch avg.	
Major Inside Dia. (new)	4.234 +/- 0.030 inch		5.234 +/- 0.035 inch	
Weight	5.9057 g		7.2809 g	
Calculated Volume	0.2038 $inch^3$ (3.340 cm^3)		0.2490 $inch^3$ (4.080 cm^3)	
Calculated Density	**1.768 g/cm^3**		**1.785 g/cm^3**	

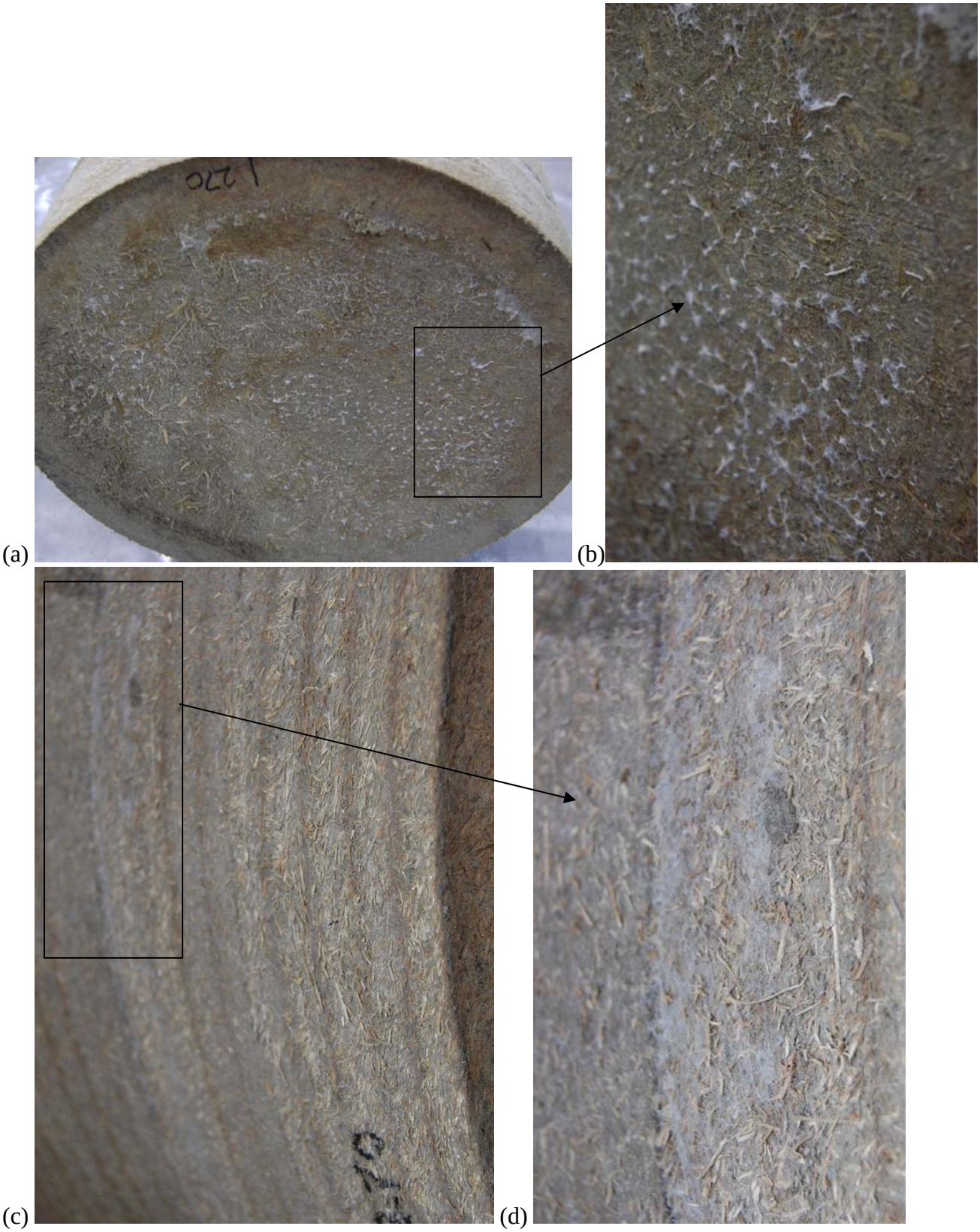

Figure 1. Mold on the bottom (a, b) and side (c, d) of lower fiberboard subassembly.

Figure 2. Mold and fiberboard residue on the inside bottom of drum.

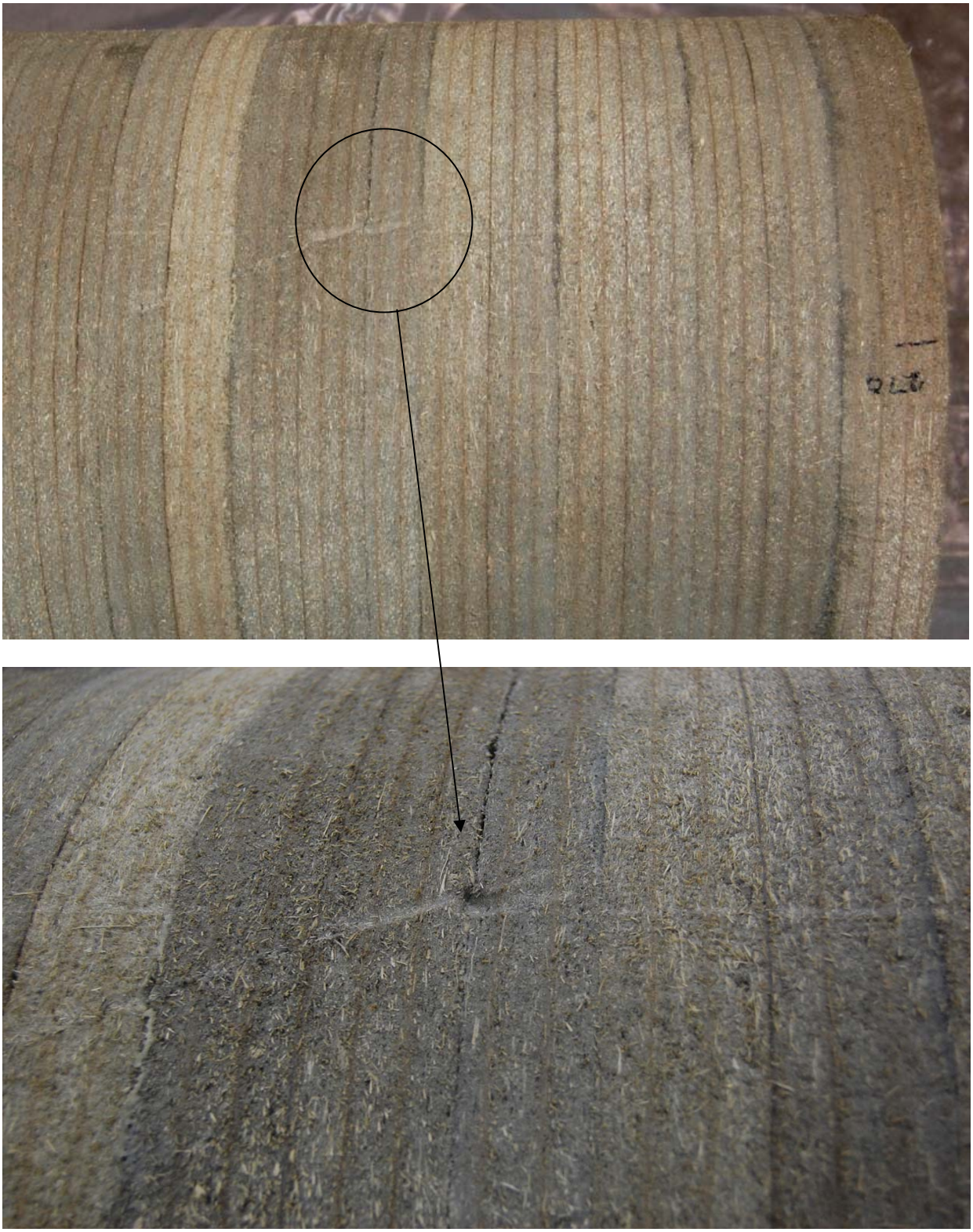

Figure 3. Scrape marks and one of two dents in the lower fiberboard OD surface, approximately 15 inches from the bottom.

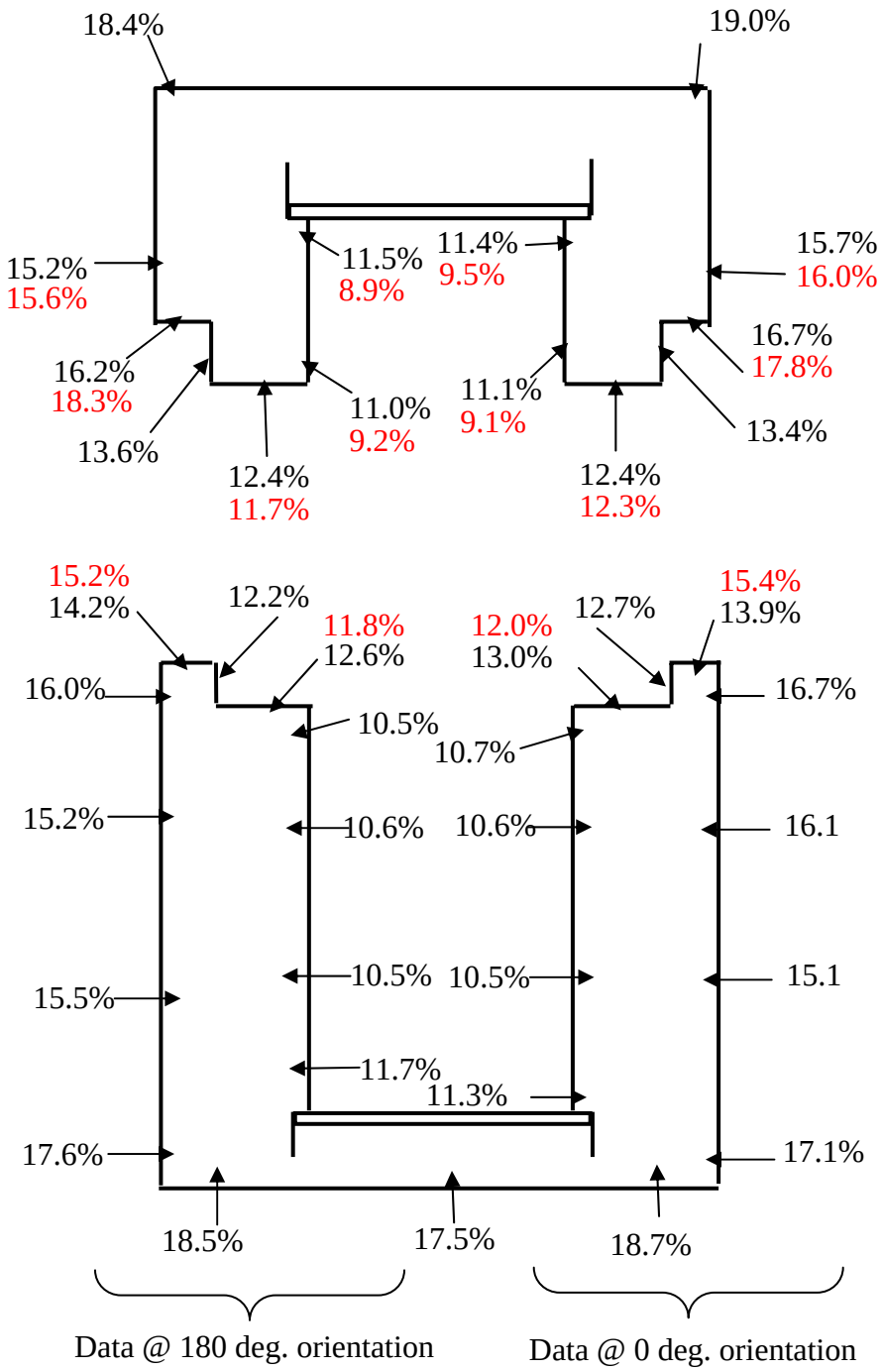

Figure 4. Fiberboard moisture content data. The values in red were measured during field surveillance. All values are % wood moisture equivalent.

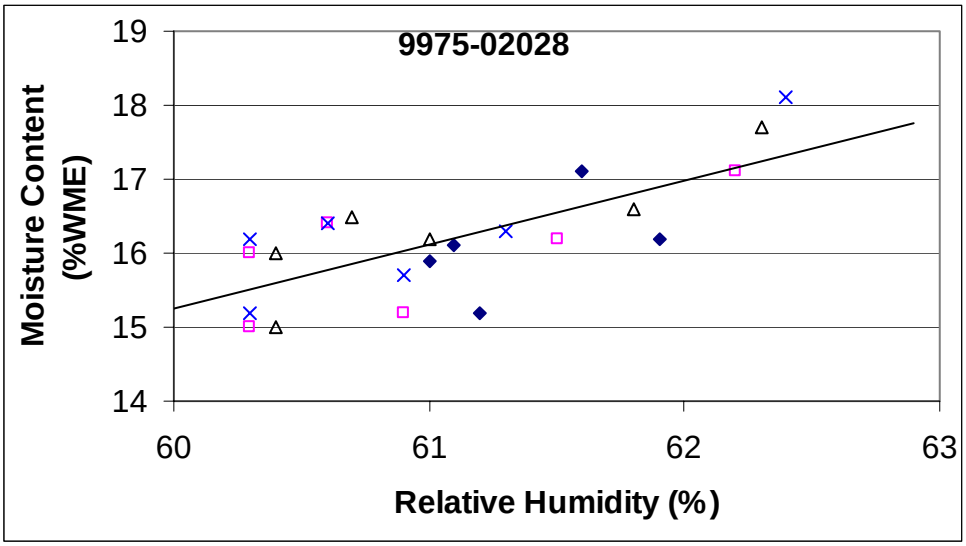

Figure 5. Correlation between fiberboard moisture content and relative humidity of the adjacent air. Measurements were taken along the fiberboard OD surface.

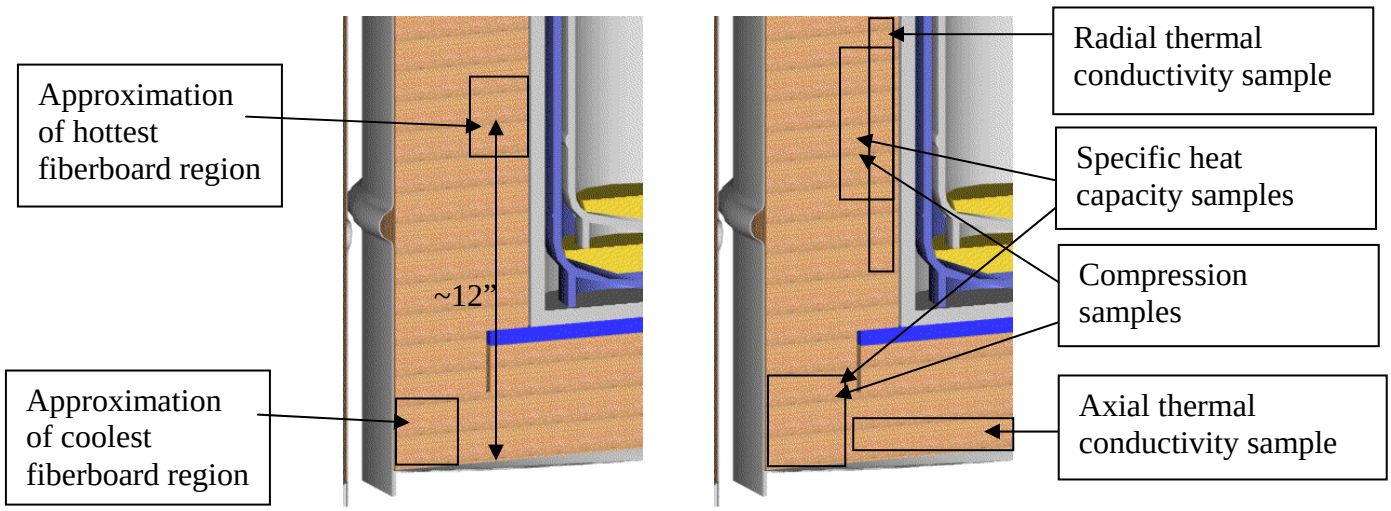

Figure 6. Illustration of fiberboard regions of the bottom subassembly to be tested. Multiple samples (where used) were removed from the illustrated locations at different circumferential positions. Not to scale.

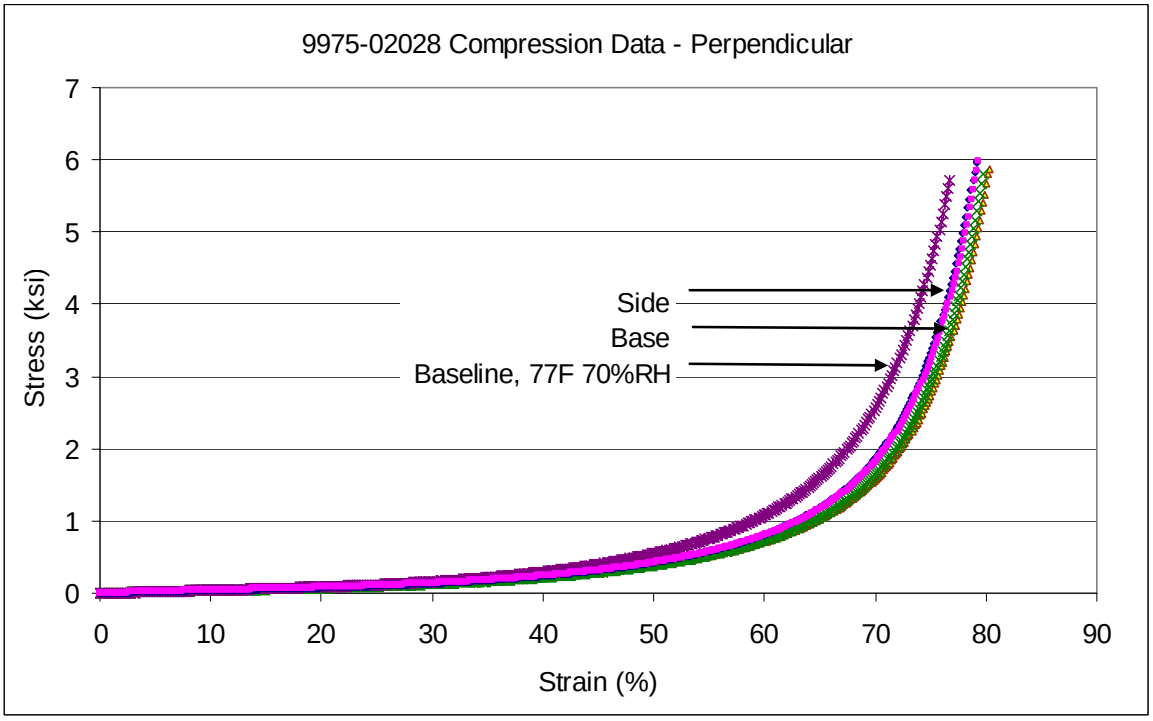

Figure 7. Fiberboard compression test data, compared with typical baseline (77°F, 70% RH) data, in the perpendicular orientation (i.e. load applied perpendicular to the fiberboard layers).

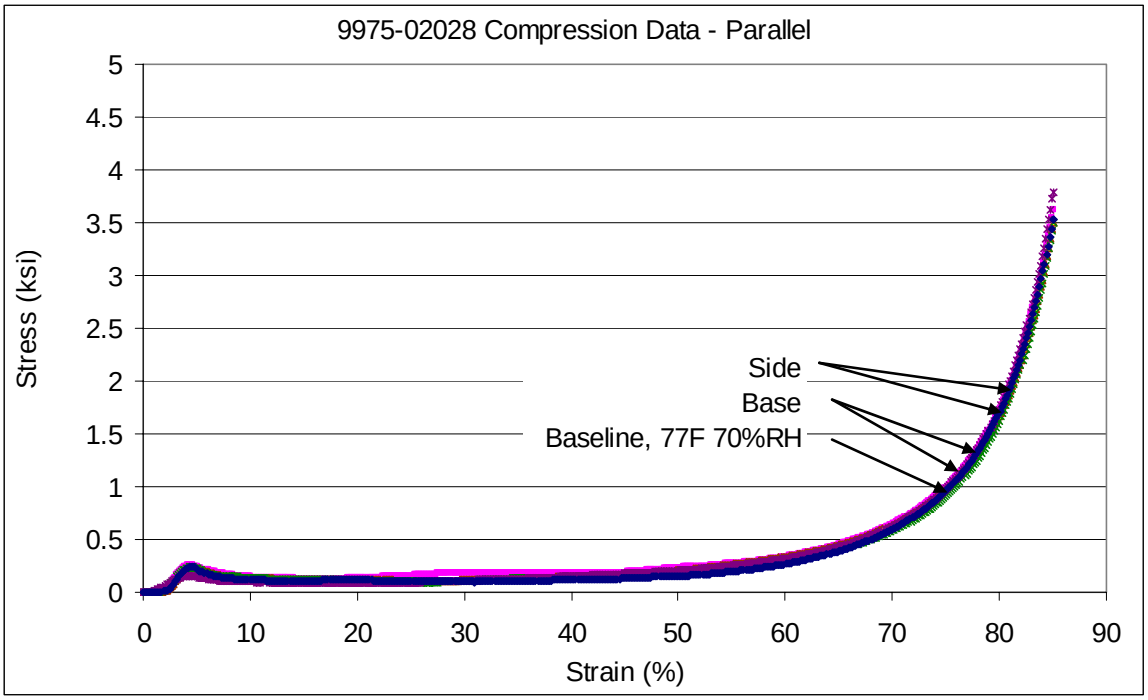

(a)

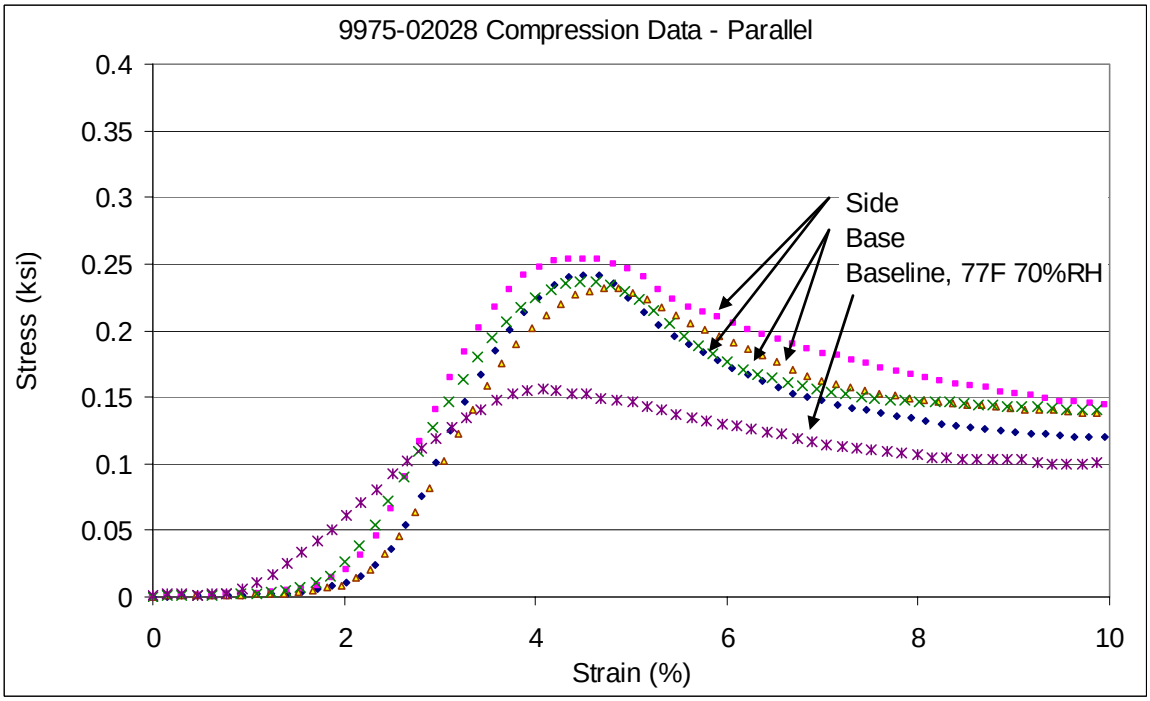

(b)

Figure 8. Fiberboard compression test data, compared with typical baseline (77°F, 70% RH) data, in the parallel orientation (i.e. load applied parallel to the fiberboard layers). The full curves are shown in (a), while the initial buckling region is expanded in (b).

(a) Sample B1 from base of subassembly (b) Sample S2 from side of subassembly

Figure 9. Photographs of fiberboard samples during compression testing, parallel orientation

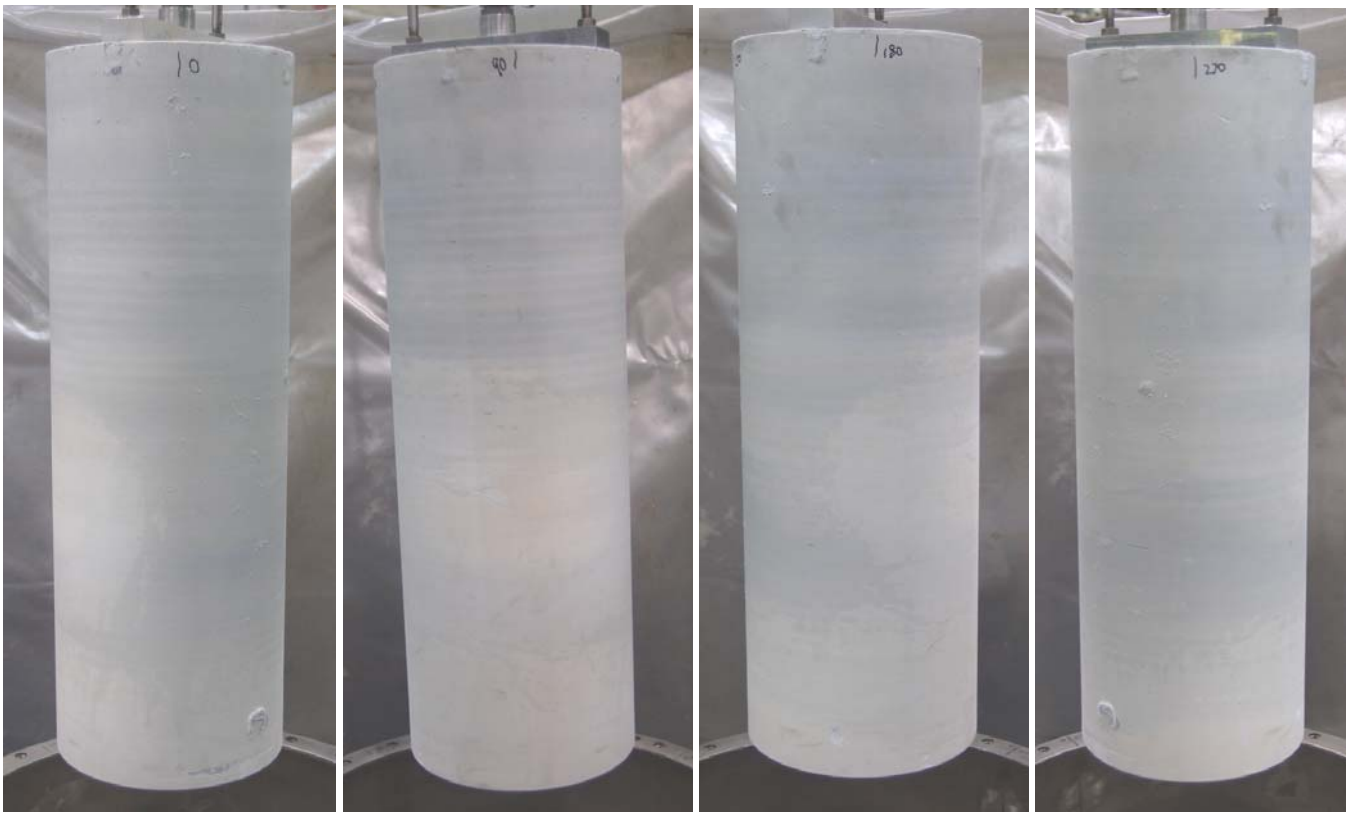

Figure 10. Lead shield with corrosion product.

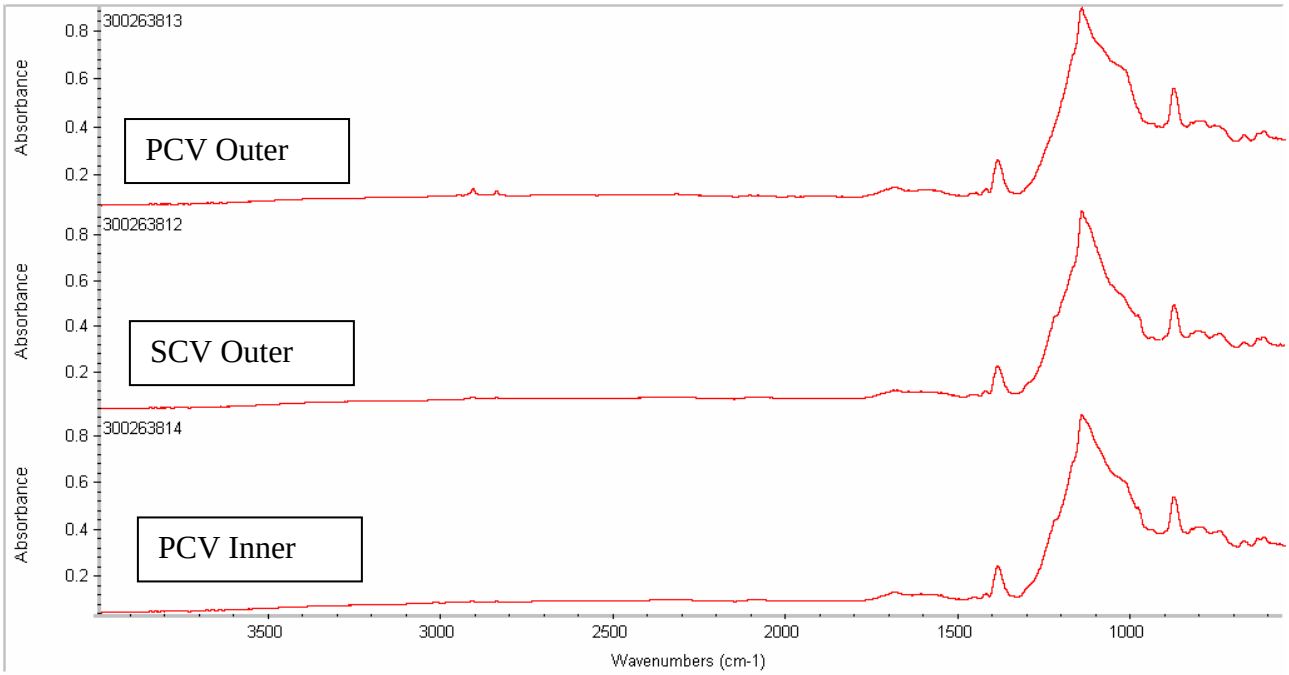

Figure 11. FT-IR spectra for the three tested O-rings. Each spectrum is consistent with a Viton® type fluoroelastomer.

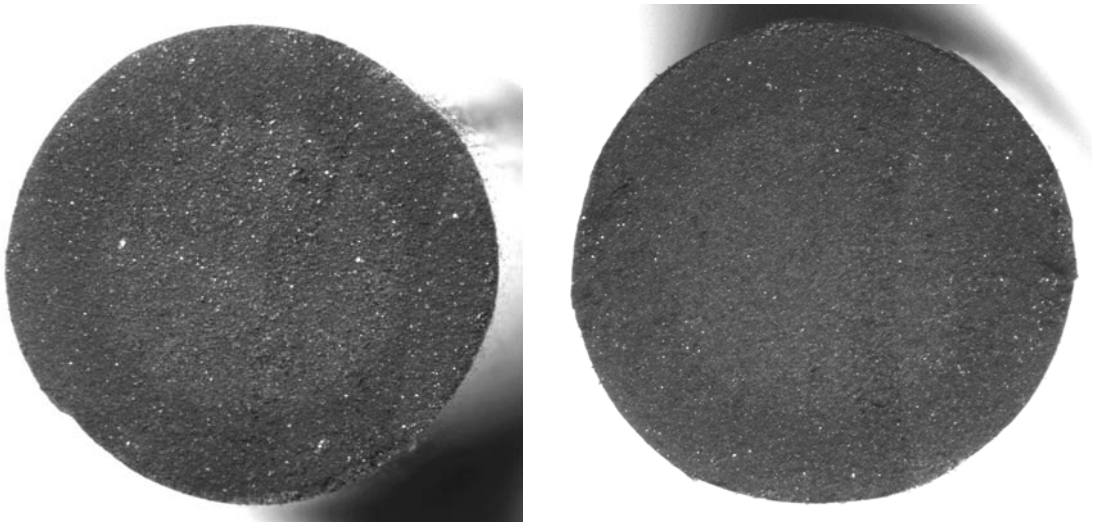

(a) (b)

Figure 12. Visual cross section of the (a) PCV outer and (b) SCV outer O-rings.

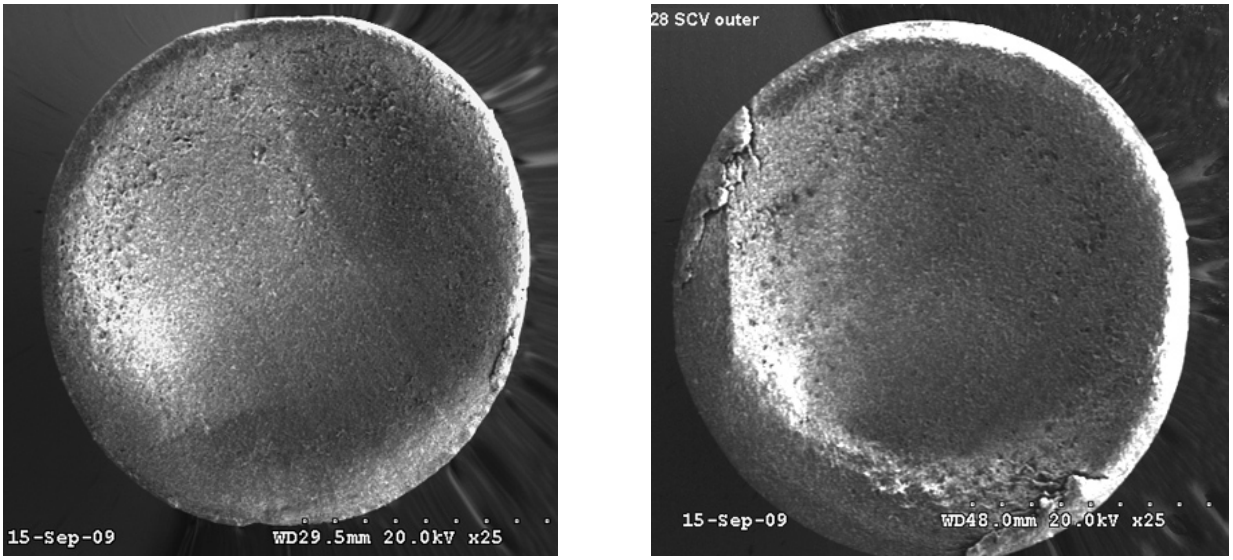

(a) (b)

Figure 13. SEM cross section of the (a) PCV outer and (b) SCV outer O-rings.

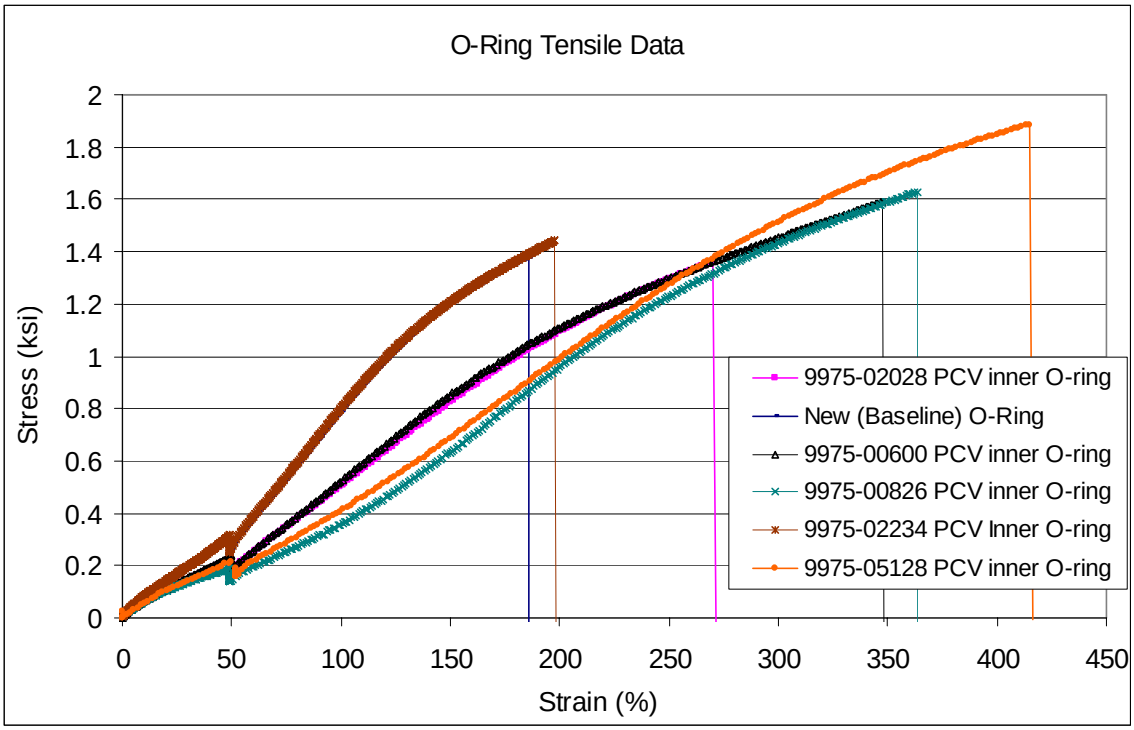

Figure 14. Tensile data for PCV inner O-ring from 9975-02028, compared to a new O-ring and the PCV O-rings from previously examined packages.

Figure 15. Small stain or superficial rust spot near bottom of PCV exterior.

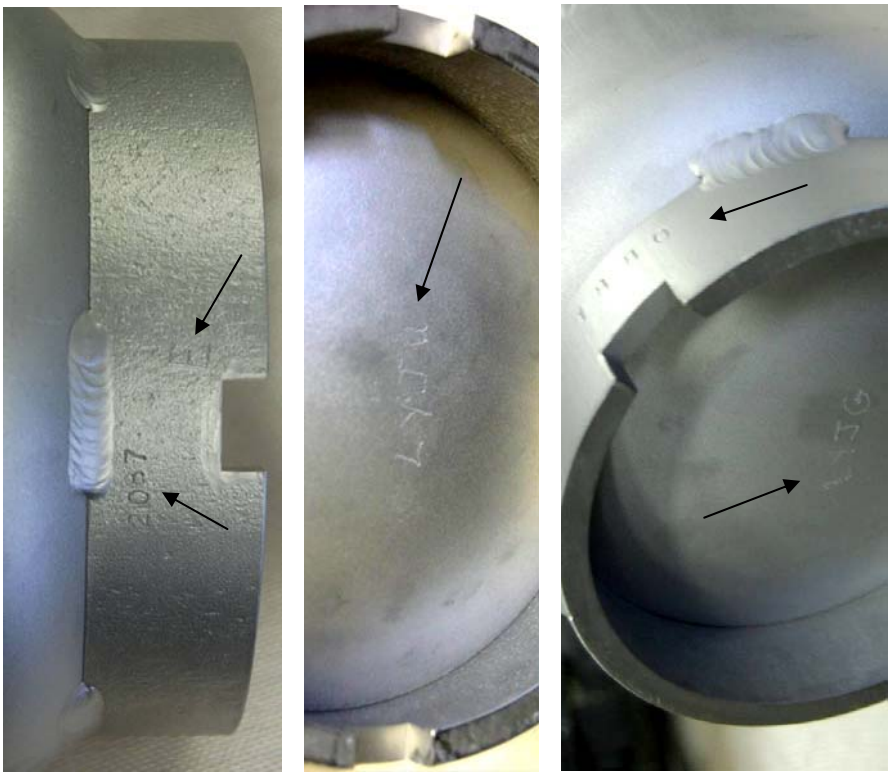

(a) (b) (c)

(d) (e) (f)

Figure 16. Fabrication markings (at arrows) on SCV (a, b), PCV (c) SCV lid (d) and PCV lid (e, f)

Attachment 1 9975-02028 Field Surveillance Results, with Comparison to Destructive Examination Results

Section I

Drum Exterior Examination

Item	Field Surveillance Result	Destructive Exam. Result
Drum vent plugs are specified and are in place as required	SAT	SAT
Drum surface is not dented beyond 0.25 inch	SAT	SAT
Drum Dents adjacent to the air shield are not deeper than 0.125 inch	SAT	SAT
Drum surface is free from corrosion, swelling/bulging and other physical damage	SAT	SAT

Section II

Temperature Measurements

[These data not repeated in this report.]

Section III

Celotex® Inspection

Upper Celotex® Assembly Weight: 26.6 lb (field surv.) 12.186 kg / 26.87 lb (destructive exam)

Visual:

Item	Field Surveillance Result	Destructive Exam. Result
Inspect all exposed Celotex® surfaces for significant damage and ensure layers are well bonded	SAT	SAT
Upper Celotex® came out smoothly, without interference	SAT	SAT
All visible Celotex® surfaces are free from staining and variation in coloration	SAT	UNSAT*
Celotex® is free from significant swelling (e.g. gap exists against drum), shrinkage and other significant physical damage	SAT	SAT
Lead shield interior is free from significant deformation and physical damage	SAT	SAT
Lead shield Go/No Go gauge went smoothly into the lead shield and reached all the way to the bottom of the lead shield	SAT	NA

* Lower fiberboard subassembly had areas of mold.

Attachment 1 9975-02028 Field Surveillance Results, with Comparison to Destructive Examination Results

Celotex® Dimensions (all results reported in inches)

Dimensions		0°	90°	180°	270°	Field Surveillance Average	Destructive Exam. Average
1	Upper Assembly OD	17.616	17.624			17.620	17.690
2	Upper Assembly lower step OD	14.673	14.674			14.674	14.658
3	Upper Assembly ID	8.527	8.532			8.529	8.543
4	Upper Assembly inside height	4.953	4.961	4.948	4.962	4.956	4.992
5	Lower Assembly step height	1.985	2.003	2.012	2.047	2.012	2.098
6	Lower Assembly height from lower step to top of lead shield	4.260	4.288	4.316	4.299	4.291	NA

Dimension	Result	Criteria	Field Surveillance Result	Destructive Exam. Result
Dimension #6 average	4.291	≤ 4.65 "	SAT	NA
Dimension #1 average – Dimension #3 average	9.091	$\geq 8\ 3/16$"	SAT	SAT

Section IV

O-Ring Inspection

Test	SAT/UNSAT
O-ring seal test performed on SCV	SAT
SCV O-rings were removed intact	SAT
SCV O-rings have no excess accumulation of grease	SAT
O-ring seal test performed on PCV	SAT
PCV O-rings were removed intact	SAT
PCV O-rings have no excess accumulation of grease	SAT

Attachment 1 9975-02028 Field Surveillance Results, with Comparison to Destructive Examination Results

(all dimensional results reported in inches)

Action	0°	90°	180°	270°	Time	Destructive Exam. Average Result
Loosen SCV lid					1017	NA
Outer SCV O-Ring						
Measure OD (while on plug)	6.277	6.286			1022/1024	NA
Measure radial thickness	0.1270	0.1315	0.1370	0.1360	1030/1031	0.1394
Measure vertical thickness	0.1250				1030	0.1355
Inner SCV O-Ring						
Measure OD (while on plug)	6.171	6.172			1025/1026	NA
Measure radial thickness	0.1255	0.1265	0.1260	0.1280	1029/1029	NA
Measure vertical thickness	0.1350				1028	NA
Loosen PCV lid					1046	NA
Outer PCV O-Ring						
Measure OD (while on plug)	5.230	5.234			1050/1051	NA
Measure radial thickness	0.1260	0.1260	0.1360	0.1260	1056/1057	0.1341
Measure vertical thickness	0.1330				1056	0.1373
Inner PCV O-Ring						
Measure OD (while on plug)	5.114	5.115			1052/1053	NA
Measure radial thickness	0.1300	0.1250	0.1330	0.1285	1054/1056	NA
Measure vertical thickness	0.1340				1054	NA

Attachment 1 9975-02028 Field Surveillance Results, with Comparison to Destructive Examination Results

SRNL Receipt Examination of O-Rings

VISUAL EXAMINATION

PCV	PCV Outer	PCV Inner
Grease present	yes	yes
Color (normal or explain)	Normal	Normal
Cross-sectional shape	round	round
Nicks, Scratches, Cracks	none	none
Other Damage (Note extent/size)	none	none
Picture (Note if taken)		

SCV	SCV Outer	SCV Inner
Grease (type, amount)	yes	yes
Color (normal or explain)	Normal	Normal
Cross-sectional shape	round	round
Nicks, Scratches, Cracks	none	none
Other Damage (Note extent/size)	none	none
Picture (Note if taken)		

THICKNESS (all results reported in inches)

PCV	PCV Outer		PCV Inner	
	Axial	Radial	Axial	Radial
Thickness 1 (in)	0.1350	0.1350	0.1350	0.1325
Thickness 2 (in)	0.1345	0.1315	0.1325	0.1375
Thickness 3 (in)	0.1325	0.1370	0.1350	0.1315
Thickness 4 (in)	0.1335	0.1360	0.1340	0.1350
Field Surv. Average	**0.1339**	**0.1349**	**0.1341**	**0.1341**
Destructive Exam Average	**0.1348**	**0.1369**		

SCV	SCV Outer		SCV Inner	
	Axial	Radial	Axial	Radial
Thickness 1 (in)	0.1330	0.1315	0.1335	0.1355
Thickness 2 (in)	0.1315	0.1380	0.1325	0.1375
Thickness 3 (in)	0.1315	0.1360	0.1360	0.1370
Thickness 4 (in)	0.1345	0.1370	0.1365	0.1365
Field Surv. Average	**0.1326**	**0.1356**	**0.1340**	**0.1366**
Destructive Exam Average	**0.1335**	**0.1375**		

Attachment 1 9975-02028 Field Surveillance Results, with Comparison to Destructive Examination Results

SRNL Receipt Examination of O-Rings (Continued)

HARDNESS

	PCV O-Rings		SCV O-Rings	
	Outer	Inner	Outer	Inner
Hardness 1, M-Scale	72.0	71.5	73.5	73.0
Hardness 2, M-Scale	72.0	72.0	73.0	74.0
Hardness 3, M-Scale	72.0	74.0	68.5	74.0
Hardness 4, M-Scale	72.0	76.0	69.0	73.0
Hardness 5, M-Scale	70.5	74.5	71.5	71.0
Average	**71.7**	**73.6**	**71.1**	**73.0**

CONTINUATION:
NA

CC: J. S. Bellamy, 773-41A
G. T. Chandler, 773-A
W. L. Daugherty, 773-A
K. A. Dunn, 773-41A
H. A. Gunter, 703-H
E. R. Hackney, 705-K
M. K. Hackney, 705-K
T. K. Houghtaling, 773-41A
N. C. Iyer, 773-41A
D. R. Leduc, 773-41A
J. W. McClard, 703-H
J. W. McEvoy, 730-4B
J. L. Murphy, 773-41A
T. E. Skidmore, 730-A
A. J. Stapf, 717-K
T. D. Woodsmall, 705-K
L. S. Yerger, 105-K
Document Control